MODELLING LAND UPLIFT RATES AND THEIR ERROR PROPAGATION

Karin Kollo[1], Martin Vermeer[2]

[1]*Estonian Land Board, Mustamäe tee 51, 10621 Tallinn, Estonia*
[1, 2]*Department of Surveying Sciences, Faculty of Engineering and Architecture,*
School of Science and Technology, Aalto University, P.O.Box 11200, FI-00076 Aalto, Finland
E-mails: [1]karin.kollo@maaamet.ee (corresponding author)

Abstract. The article describes a method for deriving the precision of a predicted land uplift value at an arbitrary terrain point which is assumed connected in height to a levelling benchmark using GNSS and a precise geoid model. We derive a statistical model for predicting the uplift rate from the existing point rates along with its empirical signal covariance function. One of our aims is a study on how a land uplift rate model and its empirical covariance function can be determined and then used for calculating changes in height over the time interval between precise levellings or GNSS heightings.

Keywords: post-glacial rebound, height system, error propagation, empirical covariance function.

1. Introduction

In the future, National Height Systems will likely be maintained by GNSS (Global Navigation Satellite System) technology. This kind of a height system together with a precise geoid model and a precise land uplift model will serve as the basis for future National Height Systems. Precise levellings will most probably not be carried out to the same extent as in the past. Long measurement time to perform complete precise levelling for one country and thus poor temporal resolution as well as high cost are the main reasons. Also, today we have permanent station networks of GNSS operating for more than 15 years.

This motivates us to study precision that can be obtained determining the postglacial land uplift rate at an arbitrary point within the Fennoscandian area, because we will want to use the already known uplift rates to project geodetic heights forward in time. In the future dynamic height system, our knowledge of land uplift will be derived from a set of stations repeatedly positioned applying precise geodetic GNSS.

If we assume uplift values obtained from GNSS to be precise enough, the question of how precise will be the uplift value predicted an arbitrary point at some distance from these known points arises. In order to find this out, one firstly should know the functional behaviour of the land uplift model. Additionally, one should know the general stochastic behaviour of local uplift deviations from this functional uplift model. These deviations can be characterized by a signal covariance function; the estimation technique to be used is least squares collocation. The signal covariance function is to be estimated empirically using a set of real-life uplift values for point pairs at a wide range of inter-point distances.

2. Post-Glacial Land Uplift

Land uplift, also called post-glacial rebound (PGR) or glacial isostatic adjustment (GIA), is caused by changes in continental ice sheet loading in high-latitude areas. It causes many significant changes in the landscape, especially near coastlines. Globally, post-glacial rebound tends to make the Earth more spherical by reducing dynamic flattening J_2 (related to the Earth's moments of inertia) over time. Nowadays, post-glacial rebound is most noticable in Fennoscandia and Canada. The maximum land uplift rate is about 1 cm per year (Ekmann 2009).

Recent land uplift in Fennoscandia has been studied for a long time. A systematic collection of measurements started by the end of the 19th century: first, mareograph records and geodetic levellings have remained as conventional tools to study land uplift. Second, the GPS technique has been widely used in land uplift determination from 1990. Relative gravity measurements have been used for many decades for determining land uplift, cf., e.g. (Mäkinen *et al.* 1985). Also, terrestrial absolute gravimetry is a further, recently becoming popular, technique for studying land uplift.
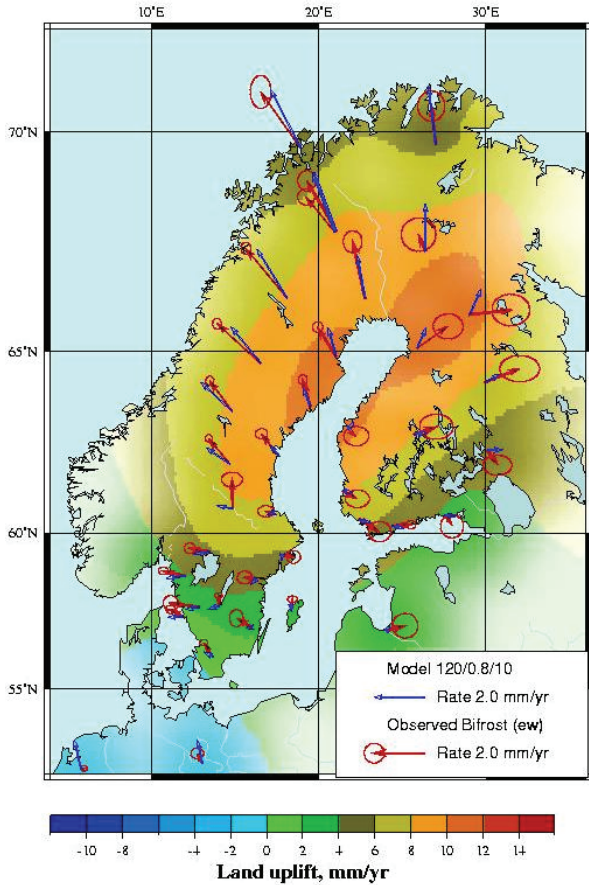
Fig. 1. BIFROST land uplift model (2001)
(Johansson *et al.* 2002)

Several land uplift models have been obtained over the last decades; one of those we mention is designed by Ekmann (1996), Lambeck *et al.* (1998) and Vestøl (2006). These models are based on the following data types: sea-level records, lake level records, repeated high-precision levellings and time series from continuous GPS stations (for the Vestøl model). In 1992, the project called BIFROST (Baseline Inferences for Fennoscandian Rebound Observations, Sea-level and Tectonics) was created (Fig. 1). It combines networks of continuously operating GNSS receivers in Fennoscandia and nearby areas to measure ongoing crustal deformation due to glacial isostatic adjustment (Johansson *et al.* 2002).

While different modelling techniques were used in these models, they all agree that the maximum uplift rate for Fennoscandia is about 10 mm/year (Ekmann 1996; Staudt *et al.* 2004; Lambeck *et al.* 1998; Vestøl 2006; Müller *et al.* 2005).

3. Modelling Method Outline and Theory

For our analysis, both GNSS-based data (Fennoscandia) and precise levelling data (Finland) were used. The used GNSS data was an existing dataset (45 points) from the BIFROST project (Johansson *et al.* 2002), cf. Fig. 2. The levelling data we used was a dataset (461 points) from the last Finnish precise levelling, jointly adjusted with the previous levelling campaigns (V. Saaranen, Finnish Geodetic Institute, personal comm.), cf. Fig. 2.
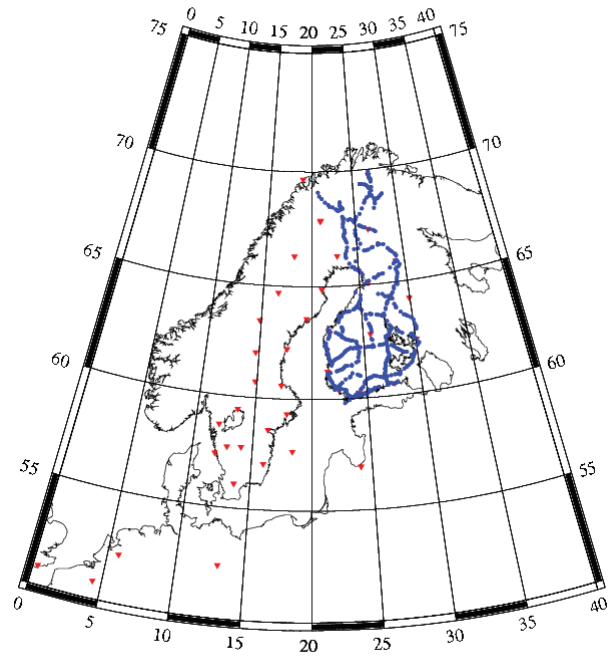

Fig. 2. Land uplift data points used in this study. BIFROST points are painted red, Finnish precise
levelling points are blue

We assumed that the geoid uplift, being at most 0.4 mm/a, may be modelled precisely enough so that its uncertainty can be neglected.

To test our hypothesis, we have built a statistical model for predicting the uplift rate at an arbitrary point in the terrain from the following given point rates:
- least-squares collocation, using 2D elliptical approximation fitted to the uplift values in the Fennoscandian area treating residuals as "signal";
- deriving an empirical covariance function for these residual uplift rates;
- using as input for collocation computation, the uplift rates from BIFROST and from Finnish precise levellings (Fig. 2).

This analysis yields the precision of the uplift rate of a predicted point anywhere in the terrain, which is height-connected to levelling benchmarks using GNSS and a precise geoid model.

3.1. Model Parametrization

We start model derivation with parametrization. First, we conjecture a simple functional model based on a bilinear function of two-dimensional location within the land uplift area:

$$\frac{dH}{dt} = f(Q). \tag{1}$$

For function *f*, we take a dual exponential or Gaussian model:

$$f(Q) = ae^{-Q} - be^{-cQ}. \tag{2}$$

This choice allows us modelling both the central uplift and the larger-area downlift, which are both known to exist.

Quadratic form Q is defined as (M being a symmetric matrix):

$$Q = \mathbf{x}^T M \mathbf{x}, \tag{3}$$

where $\mathbf{x} = [x \ \ y]^T$ is the vector of map projection plane co-ordinates centered at the maximum land uplift location. The matrix is written as:

$$M = \begin{bmatrix} m_{11} & m_{21} \\ m_{12} & m_{22} \end{bmatrix}. \tag{4}$$

Applying this model, eight unknowns to be estimated are: the elements of M, i.e., m_{11}, m_{22}, $m_{12} = m_{21}$; coefficients a, b, c; and land uplift centre location φ_0, λ_0. This is a non-linear least-squares problem.

As an alternative, "Hirvonen-style" functional model can be chosen:

$$f(Q) = \frac{a}{1+Q} - \frac{b}{1+cQ}. \tag{5}$$

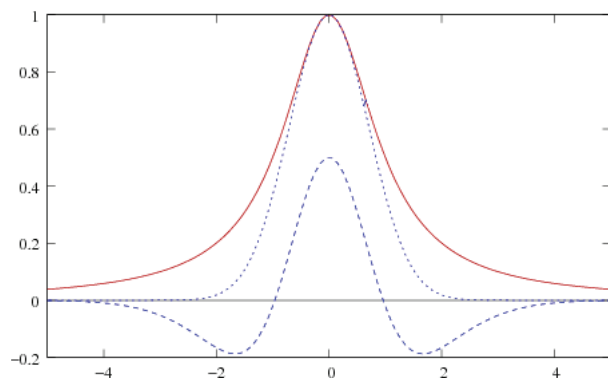Fig. 3 gives a graphical representation of the above discussed models.

Fig. 3. The cross-section shapes of the Gaussian (exponential e^{-x^2}) and Hirvonen-like $\left(\dfrac{1}{1+x^2}\right)$ model functions. Gaussian is blue, dotted, Hirvonen-like is red, drawn. Here it is assumed that $Q = x^2$, i.e., $M = I$, and $a = 1$ and $b = 0$. The third curve is composite exponential ($e^{-x^2} - 0.5e^{-0.25x^2}$), where $a = 1$, $b = 0.5$ and $c = 0.25$ illustrating our attempt at modelling both uplift and remote-zone subsidence

3.2. Map Projection Coordinates

In the definition of Q (cf. Expression (4)), it has been assumed that we have a pair of plane co-ordinates $\mathbf{x} = [x \ \ y]^T$ which have the maximum land uplift location (φ_0, λ_0) as their origin. Such coordinates are obtained by map projection, yielding for each point the following co-ordinate pair:

$$x = R\langle \mathbf{r} \cdot \mathbf{e}_N \rangle = R\sin(\varphi - \varphi_0) +$$
$$2R\cos\varphi \sin\varphi_0 \sin^2 \left[\frac{1}{2}(\lambda - \lambda_0) \right],$$

$$y = R\langle \mathbf{r} \cdot \mathbf{e}_E \rangle = R\cos\varphi \sin(\lambda - \lambda_0). \tag{6}$$

One sees that these values are scaled to the size of the Earth by multiplying with $R = 6378.137$ km.

3.3. Constructing Vectors and Matrices

Obtaining the design matrix for the computation of our unknowns requires the derivation of all partial derivatives of our "observed" quantities, i.e., uplift values, with respect to each of the unknowns.

We have the following unknowns assembled in a vector of unknowns:

$$X = [m_{11} \ \ m_{12} \ \ m_{22} \ \ a \ \ b \ \ c \ \ \varphi_0^\circ \ \ \lambda_0^\circ]^T, \tag{7}$$

units: m_{ij} in km^{-2}, a, b in mm a^{-1}, c dimensionless and $\varphi_0^\circ, \lambda_0^\circ$ in degrees.

Consequently, as design matrix A we have the following (for one observation $\dfrac{dH}{dt} = f(Q)$):

$$A = \begin{bmatrix} \dfrac{\partial f}{\partial m_{11}} & \dfrac{\partial f}{\partial m_{12}} & \dfrac{\partial f}{\partial m_{22}} & \dfrac{\partial f}{\partial a} & \dfrac{\partial f}{\partial b} & \dfrac{\partial f}{\partial c} & \dfrac{\partial f}{\partial \varphi_0^\circ} & \dfrac{\partial f}{\partial \lambda_0^\circ} \end{bmatrix}. \tag{8}$$

This matrix describes a nonlinear adjustment problem: the elements of A will contain some of the unknowns explicitly, and these should be replaced by approximate values, solving the system iteratively and re-evaluating the elements of matrix A in every step.

3.4. Linearization and Regularization

The observation equations above are highly nonlinear; it can be seen that the elements of matrix A depend upon the very unknowns we are trying to estimate. In all these expressions, values for a. b, c, m_{11}, m_{12}, m_{22}, φ_0° and λ_0° must be taken as approximate values and iteratively improved.

The linearized set of observation equations is:

$$f(Q) - f(Q_0) \approx A_0(X - X_0), \tag{9}$$

which is valid within a certain neighbourhood of X_0, i.e., $X \approx X_0$.

From this set of equations we solve:

$$X = X_0 + \left[A_0^T A_0 \right]^{-1} A_0^T (f(Q) - f(Q_0)), \tag{10}$$

where $A_0 = A(X_0)$ and $Q_0 = Q(X_0)$ are the values evaluated for the "current best" approximate unknowns X_0. Good initial values would be:

$$X_0 = \begin{bmatrix} (1000 \text{ km})^{-2} \\ 0 \\ (1000 \text{ km})^{-2} \\ (10 \text{ mm a})^{-1} \\ (1 \text{ mm a})^{-1} \\ 0.25 \\ 65^\circ \\ 24^\circ \end{bmatrix}.$$

In reality, due to the high nonlinearity of the functional model, we use attenuation factor μ slowing down but stabilizing the iteration process and regularization matrix R:

$$X = X_0 + \mu[A_0^T A_0 + R]^{-1} A_0^T (f(Q) - f(Q_0)). \quad (11)$$

4. The Functional Model Fit Computations

The BIFROST project (Johansson *et al.* 2002) provides us with geocentric land uplift $\left(\dfrac{d}{dt}h, \varphi, \lambda\right)$ values. In the dataset from the Finnish precise levellings, on the other hand, the quantity studied is land uplift relative to mean sea level, i.e., $\dfrac{d}{dt}H$. It provides locally higher point density.

We estimated the parameters of the above uplift model in order to subtract the estimated model quantities from the observed uplifts. In this case, our purpose is to obtain residual uplifts $\delta\dfrac{d}{dt}h$ so that we can derive an empirical covariance function from these residuals. When using Finnish uplift values, we would thus obtain an empirical covariance function of $\delta\dfrac{d}{dt}H$ instead.

The aim of the study was to determine uplift at a point of which the position coordinates are given. We worked with three scenarios, (cf. Fig. 4):

1. BIFROST uplift values for the whole area;
2. BIFROST uplift values for the central area only;
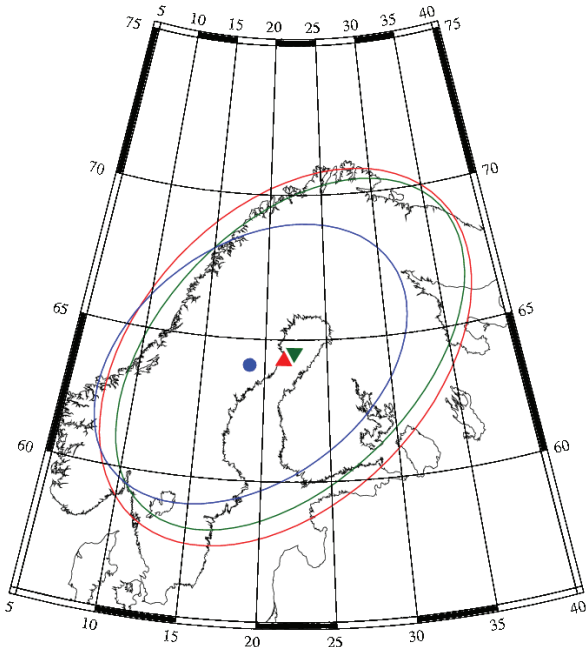3. Uplift values from the Finnish precise levelling campaigns.

Fig. 4. The best-fit ellipses found for various modelling scenarios. Red triangle: the whole BIFROST area; green inverted triangle: BIFROST central area; blue circle: the Finnish precise levelling. Note significant difference between BIFROST on the one hand and the Finnish levelling on the other, suggesting that the land uplift geometry is in reality asymmetric

For computations, we used Octave (Eaton 2002), a Matlab ™ compatible rapid prototyping language. For graphics generation, Octave, Gnuplot (http://www.gnuplot.info) and GMT (Geographic Mapping Tools (Wessel, Smith 1998)) software packages were used.

4.1. Test Computation Results

We start our computations by choosing good initial values for our unknowns. First, we fixed for the exponential model is parameter c at 0.25 (meaning the radius of the downlift area to be $2\times$ that of the uplift area) and varied Q_0. The obtained results are presented in Table 1.

Table 1. Test computation results, c = 0.25. The Root-Mean-Square error of fit and the number of rejected outliers according to 3σ test criterion are listed

Q_0	Exponential		Hirvonen	
	RMS	No. rej.	RMS	No. rej.
∞	3.616	0	3.915	0
9	3.590	1	3.875	1
6.25	**1.685**	**2**	3.875	1
4.5	–	–	1.940	3
4	1.431	6	–	–
2.25	–	–	–	–
1	0.696	18	–	–

Next, we fixed b to zero, essentially reducing the model to:

$$f(Q) = ae^{-Q} \text{ or } f(Q) = \frac{a}{1+Q}. \quad (12)$$

Results for this strategy are listed in Table 2.

Table 2. Test computation results, $b = 0$

Q_0	Exponential		Hirvonen	
	RMS	No. rej.	RMS	No. rej.
4	1.729	8	2.017	9
2.25	1.453	9	1.265	13
1.5	1.419	11	–	–
1.4	–	–	–	–
1.3	0.852	13	0.776	19
1.2	0.830	14	0.776	19
1.1	0.774	15	0.743	20
1	0.696	18	–	–

4.2. Modelling the Whole Area

From the above, one can see that when solving a function that should describe the whole land uplift area including the surrounding downlift area, a good choice is $Q_0 = 6.25$ for a two-term exponential expression, i.e., $c = 0.25$ (cf. Table 1). The RMS of residuals in this case is ± 1.685 mm a^{-1}. When fitting this function, two points, Madrid and Ny Ålesund, were excluded as they both are situated outside the Fennoscandian area. We summarize this solution below:

$$M = \begin{bmatrix} 2.1725 & -0.8706 \\ -0.8706 & 2.2786 \end{bmatrix} \cdot 10^{-6} \text{ km}^{-2},$$

$a = 14.265 \text{ mm a}^{-1}$,

$b = 2.879 \text{ mm a}^{-1}$,

$c = 0.25$,

$\varphi_0 = 64°.340$,

$\lambda_0 = 21°.500$.

The ellipse describing the uplift area has semi-axes of 859.62 and 568.17 km aimed at an azimuth of 43°.26. The maximum uplift is $a - b = 11.386$ mm/a.

4.3. Modelling the Central Area

For the central area, we derive an empirical signal covariance function of the uplift for using local uplift data. Thus, we can use a function that fits the data more precisely (RMS ±0.852 mm a^{-1}) but over a smaller area. Such a function is the one-term exponential solution (i.e., $b = 0$) for $Q_0 = 1.3$ (cf. Table 2). The summary for this solution is:

$$M = \begin{bmatrix} 2.6975 & -1.2605 \\ -1.2605 & 2.7738 \end{bmatrix} \cdot 10^{-6} \text{ km}^{-2},$$

$a = 11.341 \text{ mm a}^{-1}$,

$b = 0$,

$c = \text{irrelevant}$,

$\varphi_0 = 64°.459$,

$\lambda_0 = 21°.866$.

The ellipse describing the uplift area has semi-axes of 823.87 and 500.28 km aimed at an azimuth of 44°.10.

4.4. Modelling the Finnish Precise Levelling Based Uplift Values

We also derive an empirical signal covariance function for the Finnish precise levelling based uplift values, obtaining the following exponential solution for $Q_0 = 1.3$:

$$M = \begin{bmatrix} 3.7321 & -1.2630 \\ -1.2630 & 3.2075 \end{bmatrix} \cdot 10^{-6} \text{ km}^{-2},$$

$a = 9.586 \text{ mm a}^{-1}$,

$b = 0$,

$c = \text{irrelevant}$,

$\varphi_0 = 64°.091$,

$\lambda_0 = 18°.7649$.

The RMS of the residuals of being fit was ±0.314 mm/a, which compares well to the known precision of ±0.4 mm/a of the Finnish precise levelling uplift values (Mäkinen *et al.* 2003), but which may be contrasted with the corresponding, much larger values derived

above from BIFROST data. This suggests that the chosen functional models are not well able to precisely model the land uplift over so large area.

The ellipse describing the uplift area for the Finnish solution has semi-axes of 677.30 and 458.36 km respectively, with the long axis pointing at the azimuth of 50°.866.

Compared to BIFROST solution, some differences can be noticed. The land uplift maximum is 9.586 mm/a, which is clearly less than BIFROST value, by an amount (1.755 mm/a for the central area solution) fully explainable by rise in the mean sea level in the Baltic Sea relative to the geocentre.

5. Empirical Covariance Function Estimation

After estimating a functional model for the land uplift, as done above, one can then derive, using least-squares collocation, uncertainty over the Fennoscandian area. For this purpose, one can use the land uplift values estimated from the values known at a number of discrete points, i.e. EUREF stations, for which the precise GNSS-derived land uplift is known. To this end, we first must derive an empirical covariance function for residuals relative to the functional model.

Once we have obtained, for each of land uplift data points $\left(\dfrac{d}{dt} h, \varphi, \lambda \right)$ used in the computation, residuals $\delta \dfrac{d}{dt} h$ relative to the functional model, we can estimate the empirical covariance function as follows:

1. For each pair of uplift points P an Q, determine product $\delta \dfrac{d}{dt} h_P \cdot \delta \dfrac{d}{dt} h_Q$.
2. Determine the distance between P and Q, and choose for the above product an appropriate distance range (e.g. range 1 is $0 \leq d < 100$ km, range 2 is $100 \text{ km} \leq d < 200$ km, etc.).
3. For every range, estimate empirical covariance for this distance range $C(d)$.
4. Plot graphically covariance function $C(d)$ against d.

The procedure described assumes isotropy, i.e. the covariance function will only depend on inter-point distance, not direction, and homogeneity, i.e. we derive a function that applies unchanged to the whole area.

The described algorithm was implemented in Octave; the received results are shown in Figures 5 and 6.

Precision of Covariance Functions

As seen from Fig. 5, the covariance function for Finnish levelling (Fig. 5, right) is smooth, and the part close to the origin resembles the ideal of a bell-shaped curve. For BIFROST model (Fig. 5, left), one can see that the covariance function does not look quite as nice: the curve lies everywhere inside its 3σ uncertainty bounds, which are very wide.

Fig. 6 presents standard deviation figures for BIFROST data (left) and the Finnish levelling data (right). On the horizontal axis, we have distance in kilometres, and on the vertical axis, the standard deviation (estimation uncertainty) value in millimetres for uplift per year. In Table 3, signal standard deviation values at the origin, $\sqrt{C_0}$, for two tested models (BIFROST and Finnish levelling) are presented.
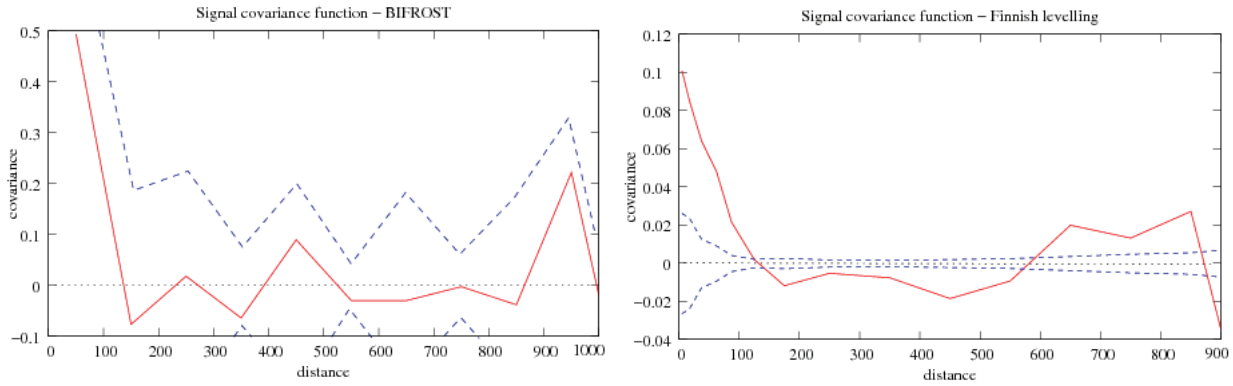
Fig. 5. Signal covariance functions (red, drawn) for tested data sets. Units: $(mm/a)^2$.
3σ bounds for standard deviation (cf. Fig. 6) are drawn in dashed blue
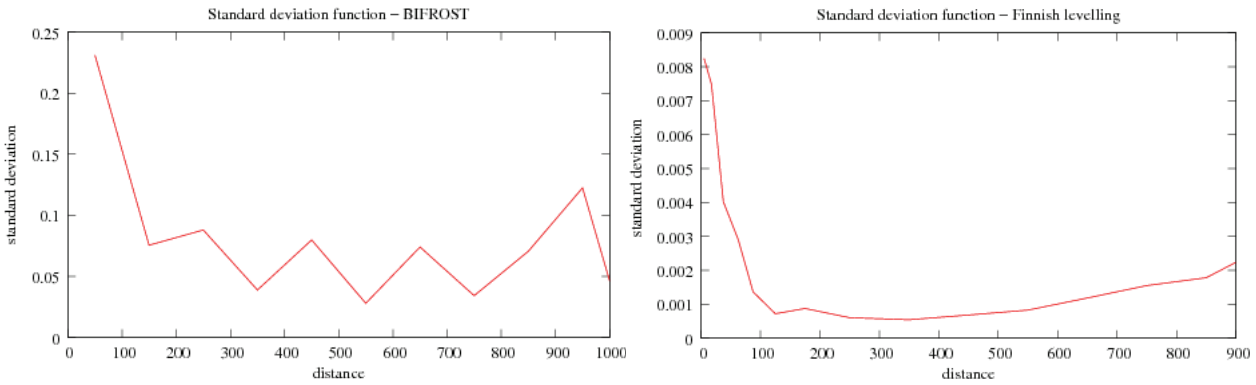

Fig. 6. Standard deviation functions for the covariance estimator functions of the tested data sets. These functions represent statistical uncertainty using which empirical covariance values presented in Fig. 5 were obtained. Units: $(mm/a)^2$

Table 3. Signal standard deviation values $\sqrt{C_0}$ for tested data sets

	Signal variance	Std. deviation
Data set	C_0 (mm/a)^2	$\sqrt{C_0}$ (mm/a)^2
BIFROST	0.558	0.75
Finnish levelling	0.099	0.31

We first discuss the BIFROST model. Standard deviation (Fig. 6) first decreases from more than 0.2 mm/a down to 0.07 mm/a for a range of about 100 km. This is understandable, because BIFROST dataset contains only long and very long distances between model points - there are not any short distances that could serve to define the curve close to the origin. For distances larger than 100 km, the standard deviation value remains small, zigzagging within the range of 0.05...0.1 mm.

Table 3 shows that the standard deviation value at the origin, $\sqrt{C_0}$ for the BIFROST model is about 0.75 mm/a. Signal covariance C_0, however, is 0.558 (mm/a)^2, which, compared to its own estimated standard deviation of 0.23 (mm/a)^2 (Fig. 6, left) amounts to only 2.4σ. The value thus differs from zero, but not in high confidence.

For the Finnish precise levelling model, the situation looks rather different. For this case, shorter distances

are more common. We can see that the scale range of the standard deviation is below 0.01 mm/a for the vertical axis. For longer distances, the standard deviation of the covariance estimate drops below 0.001 mm/a, and then increases again, but not exceeding the value of 0.0025 mm/a.

Signal standard deviation at the origin $\sqrt{C_0}$ is about 0.31 mm/a (Table 3); this value is the result of the known high precision of levelling and relatively short distances between the measured points. The signal variance C_0 of 0.099 (mm/a)^2, compared to its own standard deviation estimation of 0.0083 (mm/a)^2 (Fig. 6, right), corresponds to no less than 12 sigmas.

To conclude this discussion, one can notice that Fig. 5 and Fig. 6 are very different in nature. This is understandable, because considering BIFROST data, longer distances are common within a small amount of data points, while in the Finnish levelling, the situation is different.

For BIFROST dataset, the points of the covariance curve passest the first zero crossing are statistically insignificant. For the Finnish precise levelling dataset, however, the points containing negative values pastses the first zero crossing 120 km appear significant, and in fact, the whole curve does.

6. Using a Semi-Empirical Gauß-Markov Covariance Function

As noted above, the derived covariance function curves (Fig. 5) are suffering from considerable uncertainty (Fig. 6), especially for larger distances between point pairs. For this reason, it is probably justified to assume that a true covariance function will be close to a simple "bell curve". This results from Gauß-Markov process characterized by only two parameters: variance in origin C_0 and correlation length d_0. From a visual inspection of levelling results presented in Fig. 5, correlation length, defined as half-height inter-point distance where $C(d_0) = \frac{1}{2} C_0$, of some 70 km appears reasonable. Unfortunately, a visual inspection of BIFROST results gives no clear value but is compatible with the value of 70 km. Therefore, we define a semi-empirical covariance function as follows, choosing a second order Gauß-Markov process:

$$C(d) = C_0 \exp(-d^2 / d_0^2). \tag{13}$$

Using this function, we may predict uplift values using the least-squares collocation starting from a set of points with the known uplift values: if estimated quantity is the deviation of the uplift rate from the functional model, we then have:

$$\delta \frac{dh_P}{dt} = C_{Pi} C_{ij}^{-1} \delta \frac{dh_j}{dt}. \tag{14}$$

As this is homogeneous prediction, i.e. we are predicting the same type of quantity and uplift rate as that we are using as data, in practice, it is only data points near the prediction point that affect the result. Data points that are "behind" a closer-by data point in the same direction receive zero weight in the solution. This makes it fully justified to shortcut computation by using, e.g. only the nearest data point in each of the four quadrants surrounding the prediction point. As a practical side benefit, one also avoids having to model the, quite possibly significant, part of the signal covariance function passet the first zero crossing.

For choosing a data point set for computing the underlying functional model, it can be seen from the above that using a point set from a smaller area will lead to a more precise fit and a smaller value of C_0. This again will result in smaller residuals overall, and better quality land uplift predictions. Ideally, the residuals should represent actual uncertainty in the determination of the land uplift values in the data points; however, if the area chosen for fit is too large and the function is too simple, they will instead represent insufficiency for the fit function, which is not desirable.

7. Conclusions

Our analysis illustrates the possibilities of uplift modelling using the least squares collocation (LSC) method that was applied by (Vestol, 2006) and the results of which are considered a standard for uplift modelling within the Nordic community.

In our research, we derived, relative to simple functional models, the estimates of the signal covariance functions of land uplift residuals as well as standard deviation functions describing their estimation precision for each of two input datasets.

From our model computations we obtained an RMS value for the residuals of fit of ± 0.314 mm/a for the Finnish precise levelling model. For BIFROST, we obtained an RMS of the residuals of fit of about ± 0.852 mm a^{-1} for the central area and ± 1.685 mm a^{-1} for the whole area model. This difference may indicate that the chosen relatively simple functional model may not be sufficient to model the land uplift when using BIFROST data, especially when extending the model over the whole area.

We have shown that our analysis may be used in principle to project the land uplift rate forwarded in time. The proposed model is relatively simple and can be used for the future height systems in order to predict land uplift values in GIA regions.

References

Eaton, J. W. 2002. *GNU Octave Manual. Network Theory Limited.*

Ekman, M. 1996. A consistent map of the postglacial uplift of Fennoscandia, *Terra Nova* 8(2): 158–165.
doi:10.1111/j.1365-3121.1996.tb00739.x

Ekman, M. 2009. *The changing level of the Baltic Sea during 300 years: A clue to understanding the earth*: Technical report, Summer Institute for Historical Geophysics, Åland Islands.

Johansson, J. M.; Davis, J. L.; Scherneck, H.-G.; Milne, G. A.; Vermeer, M.; Mitrovica, J. X.; Bennett, R. A.; Elgered, G.; Elósegui, P.; Koivula, H.; Poutanen, M.; Rönn äng, B. O., and Shapiro, I. I. 2002. Continuous GPS measurements of postglacial adjustment in Fennoscandia, 1. Geodetic Results, *J. Geophys. Res.* 107: B8. doi: 10.1029/2001JB000400

Lambeck, K.; Smither, C., and Ekman, M. 1998. Tests of glacial rebound models for Fennoscandia based on instrumented sea- and lake-level records, *Geophys. J. Int.* 135: 375–387.
doi:10.1046/j.1365-246X.1998.00643.x

Mäkinen, J.; Ekman, M.; Midtsundstad, A., and Remmer, O. 1985. *The Fennoscandian land uplift gravity lines 1966–1984*. Report 85: 4. Finnish Geodetic Institute, Helsinki.

Mäkinen, J.; Koivula, H.; Poutanen, M., and Saaranen, V. 2003. Vertical velocities in Finland from permanent GPS networks and from repeated precise levelling, *Journal of Geodynamics* 35: 443–456.
doi:10.1016/S0264-3707(03)00006-1

Müller, J.; Neumann-Redlin, M.; Jarecki, F.; Timmen, L.; Denker, H., and Gitlein, O. 2005. Gravity Changes in Fennoscandian Land Uplift Area as Observed by GRACE, *Geophysical Research Abstracts* 7: 04900.

Staudt, M.; Kallio, H., and Schmidt-Thome, P. 2004. Modelling a future sea level change scenario affecting the spatial development in the Baltic Sea Region – First results of the SEAREG project, in Löser, G. S. N. (Ed.). *Managing the Baltic Sea. Coastline Reports* 2: 195–199.

Vestøl, O. 2006. Determination of Postglacial Land Uplift in Fennoscandia from Levelling, Tide-gauges and Continuous GPS Stations using Least Squares Collocation, *Journal of Geodesy* 80(5): 248–258. doi:10.1007/s00190-006-0063-7

Wessel, P., and Smith, W. F. 1998. New, improved version of Generic Mapping Tools released, *EOS Transactions of the AGU* 79: 579. doi:10.1029/98EO00426

Karin KOLLO. Chief Specialist, Department of Geodesy, Estonian Land Board, Mustamäe tee 51, 10621, Tallinn, Estonia, Ph +372 6 650 674, Fax +372 6 650 604, e-mail: *karin.kollo@ maaamet.ee.*

Post-graduate student in Aalto University, School of Science and Technology, Faculty of Engineering and Architecture, Department of Surveying

Research interests: GNSS, geoid, satellite gravimetry, geodynamics.

Martin VERMEER. Prof., PhD. Aalto University, School of Science and Technology, Department of Surveying, Ph +358 9 4702 3910, P.O. Box 11000, FI-00076 Aalto, Finland, e-mail: *martin.vermeer@tkk.fi.*

Author of over 60 scientific papers, 24 peer reviewed.

Research interests: geoid, GPS, co-ordinate systems and geodynamics, geodetic software and numerics.